Petroleum Science xxx (xxxx) xxx

Contents lists available at ScienceDirect

Petroleum Science

journal homepage: www.keaipublishing.com/en/journals/petroleum-science

Original Paper

Polymer efficiency and sulfate concentration for hybrid EOR application to an acidic carbonate reservoir

Yeonkyeong Lee [a], Wonmo Sung [b], Jihoon Wang [b, *]

[a] Korea Institute of Geoscience and Mineral Resources, 124 Gwahak-ro, Yuseong-gu, Daejeon, 34132, Republic of Korea
[b] Department of Earth Resources and Environmental Engineering, Hanyang University, 222 Wangsimni-ro, Seongdong-gu, Seoul, 04763, Republic of Korea

ARTICLE INFO

Article history:
Received 2 March 2022
Received in revised form
16 November 2022
Accepted 17 November 2022
Available online xxx

Edited by Yan-Hua Sun

Keywords:
Polymer efficiency
Low-salinity polymer flooding
Polymer adsorption
Wettability alteration
Sulfate ion
Acidic carbonate reservoir

ABSTRACT

Polymers play an important role in hybrid enhanced oil recovery (EOR), which involves both a polymer and low-salinity water. Because the polymer commonly used for low-salinity polymer flooding (LSPF) is strongly sensitive to brine pH, its efficiency can deteriorate in carbonate reservoirs containing highly acidic formation water. In this study, polymer efficiency in an acidic carbonate reservoir was investigated experimentally for different salinity levels and SO_4^{2-} concentrations. Results indicated that lowering salinity improved polymer stability, resulting in less polymer adsorption, greater wettability alteration, and ultimately, higher oil recovery. However, low salinity may not be desirable for LSPF if the injected fluid does not contain a sufficient number of sulfate (SO_4^{2-}) ions. Analysis of polymer efficiency showed that more oil can be produced with the same polymer concentration by adjusting the SO_4^{2-} content. Therefore, when river water, which is relatively easily available in onshore fields, is designed to be injected into an acidic carbonate reservoir, the LSPF method proposed in this study can be a reliable and environmentally friendly method with addition of a sufficient number of SO_4^{2-} ions to river water.
© 2022 The Authors. Publishing services by Elsevier B.V. on behalf of KeAi Communications Co. Ltd. This is an open access article under the CC BY-NC-ND license (http://creativecommons.org/licenses/by-nc-nd/4.0/).

1. Introduction

Polymers have been employed in various fields and industries to improve the efficiency of energy storage and production. In terms of energy storage, polymers are utilized for development of solar cells and batteries as an emerging technology (Qian et al., 2021; Bella et al., 2020). Polymer-based batteries have several advantages: high power densities can be achieved, flexible batteries can be developed, and recycling is possible as they are metal-free (Hager et al., 2020). In the oil and gas industry, polymers are commonly used to enhance the production of hydrocarbon fuels (Khalil et al., 2017). Adding polymers into the injection fluid increases the fluid viscosity and decreases the fluid permeability, ultimately improving the mobility of oil (Sheng, 2011).

Polymer flooding has been adopted as a mature enhanced oil recovery (EOR) method with successful outcomes in the field (Sorbie, 1991; Standnes and Skjevrak, 2014). For the injected polymer, 92% of the reported projects used partially hydrolyzed polyacrylamide (HPAM) due to its high water solubility (Standnes and Skjevrak, 2014; Sheng et al., 2015). Because the rheological properties of the HPAM strongly depend on brine salinity, low-salinity polymer flooding (LSPF) was recently proposed to improve polymer stability (Shiran and Skauge, 2013). The LSPF method has received great attention due to the synergistic effects of polymer flooding and low-salinity waterflooding (LSWF) (Vermolen et al., 2014). Lowering the salinity of the injection fluid not only prevents polymer retention (Unsal et al., 2018), but also alters the wettability of the rock surface from oil-wet to water-wet (Khorsandi et al., 2016). When low-salinity water is used as the injection fluid, it requires a smaller amount of polymer to obtain the target viscosity, which may reduce the injected polymer volume and the cost for the produced water treatment (Shiran and Skauge, 2013; Vermolen et al., 2014).

The LSPF application has practical limitations, especially for carbonate reservoirs. Most polymer flooding projects have been carried out in sandstone reservoirs due to the harsh conditions of carbonate reservoirs such as heterogeneity and low permeability (Sheng et al., 2015). In particular, the LSPF process in the United Arab Emirates (UAE) is more challenging as the carbonate oil fields have high temperature, high salinity, and high concentrations of divalent ions (Masalmeh et al., 2019). In addition, some reservoir

* Corresponding author.
E-mail address: jihoonwang@hanyang.ac.kr (J. Wang).

https://doi.org/10.1016/j.petsci.2022.11.012
1995-8226/© 2022 The Authors. Publishing services by Elsevier B.V. on behalf of KeAi Communications Co. Ltd. This is an open access article under the CC BY-NC-ND license (http://creativecommons.org/licenses/by-nc-nd/4.0/).

Please cite this article as: Y. Lee, W. Sung and J. Wang, Polymer efficiency and sulfate concentration for hybrid EOR application to an acidic carbonate reservoir, Petroleum Science, https://doi.org/10.1016/j.petsci.2022.11.012

Abbreviations

DSW	Diluted sea water
EOR	Enhanced oil recovery
FW	Formation water
HPAM	Partially hydrolyzed polyacrylamide
IW	Injection water
LSPF	Low-salinity polymer flooding
LSWF	Low-salinity waterflooding
LWALP	Low-salinity waterflooding after low-salinity polymer flooding
PV	Pore volume
PVI	Pore volume injected
RW	River water
RB	Rock–brine
ROB	Rock–oil–brine
SW	Sea water
SEM	Scanning electron microscope
TDS	Total dissolved solids
UV-Vis	Ultraviolet-visible spectroscopy
XRD	X-ray diffraction
XRF	X-ray fluorescence

fluid contains CO_2 and H_2S, which can lower the pH of the formation water. Zhu et al. (2017) reported carbonate reservoirs containing high H_2S content in the Sichuan, Tarim and Bohai Bay basins, with an observed pH of the formation water in the Halahatang area of Tarim basin, China, ranging from 5.24 to 7.2, i.e. it is mostly acidic. Thyne and Brady (2016) found that the *in-situ* pH value in carbonate and shale reservoirs of the Bakken formation in the Williston basin, Canada, ranges from 3.75 to 6.75. When the polymer is injected into low-pH conditions, its efficiency can suffer significantly, which may negatively affect the LSPF performance. Al-Anazi and Sharma (2002) investigated the rheological properties of polymer solution with respect to the effect of pH and concluded that reduction of the pH causes a decrease of polymer viscosity. According to Choi et al. (2010), the polymer becomes unstable as the polymer chains become coiled under low pH, increasing polymer adsorption. Lee et al. (2019) investigated the LSPF efficiency in a carbonate reservoir according to ion composition, ion concentration, and pH of the injection water.

However, few previous studies have investigated the effect of the acidity of formation water for applicability of the LSPF, especially in a carbonate reservoir that contains acidic formation water. When LSPF is adopted in an acidic carbonate reservoir, the polymer adsorption can be aggravated and the wettability alteration can be hindered. Consequently, the LSPF efficiency might be severely deteriorated, leading to increases in required volume of polymer and operational cost. In order to solve these problems, proper design of the injection fluid is necessary for the acidic carbonate reservoir.

In these aspects, the primary goal of this study is to investigate polymer efficiency during LSPF for an acidic carbonate oil reservoir. A set of coreflooding experiments was performed by injecting low-salinity water-based polymer solutions with various levels of salinity and SO_4^{2-} concentration into a carbonate core saturated with acidic or neutral formation water. First, the polymer retention and permeability reduction phenomena by polymer adsorption were analyzed by the measured pressure difference and ultraviolet-visible spectroscopy measurement. The wettability alteration was also investigated by changes of relative permeability and contact angle. Finally, we evaluated the enhanced oil production compared to polymer efficiency when low-salinity polymer solutions were injected into a carbonate reservoir containing acidic formation water.

2. Materials

2.1. Rock properties and preparation

The cores prepared for this study are the Desert Pink carbonate from the Edwards Plateau in Texas, USA. They were shaped and smoothed to a diameter and length of 3.81 and 12.7 cm, respectively. Fig. 1a shows the X-ray diffraction (XRD) result, indicating that the core consisted of 100% $CaCO_3$. The X-ray fluorescence (XRF) analysis, which is one of the qualitative and quantitative elemental analysis methods, indicated that the Ca^{2+} content was much higher than the Mg^{2+} content, implying that the core had not been dolomitized (Table 1). According to SEM images of the calcite core reported by Lee et al. (2019), the $CaCO_3$ crystals were close to spherical in shape (Fig. 1b). Routine core analysis of eight cores demonstrated a pore volume of 35–46 cm^3, porosity of 25%–33%, and permeability of 35–46 mD (Table 2).

In order to reconstruct the initial reservoir condition (oil-wet state), all the cores were aged with formation water and crude oil prior to the coreflooding experiments based on procedures suggested by Park et al. (2018). The cores were cleaned with deionized water, dried at 90 °C, and saturated with formation water. Crude oil was flooded through the cores until no water drained. The saturated cores were placed in aging cells for 4 weeks under a constant temperature and pressure of 90 °C and 14.7 psia, respectively.

2.2. Fluid properties and preparation

The crude oil for the experiments was obtained from an oil field in the UAE. The oil gravity was 32.7° API, and the viscosity was 5.75 cP at 60 °C (Table 3). The ionic compositions and concentrations of the formation water and injection water for the experiments are listed in Table 4. The formation water was prepared such that its composition was identical to that of water in the Middle East reservoir, with total dissolved solids (TDS) of 150,000 ppm and pH 3 (based on a confidential "water analysis report"). For the injection water, three water types with different salinity levels were prepared with an assumption that the most common and easily available water types are river water (RW), sea water (SW) and diluted sea water (DSW). The RW and SW were prepared to be compositionally equivalent to the world average river water (Behling et al., 2002) and Persian Gulf sea water (Gupta et al., 2011), respectively. As a result, the TDS of RW and SW were 120 and 35,000 ppm, respectively. The SO_4^{2-} concentrations were 10 ppm for RW and 3,000 ppm for SW. It was assumed that the TDS and SO_4^{2-} concentrations of the sea water were greatly diluted, and that DSW contained 5,000 ppm TDS and 500 ppm SO_4^{2-} ions. After preparing the synthetic brines, the measured pH of the three water types at room temperature and pressure was about 7.

For the polymer, HPAM (Flopaam 3330S™ of SNF Floerger) was selected, with a molecular weight of 8 million Da and a degree of hydrolysis of 25%–30%. Once the injection water was prepared by dissolving Na_2SO_4, $CaCl_2$, and NaCl in 1,000 mL of deionized water with a magnetic stirrer, the dried polymer was slowly added to the vortex wall created by the magnetic stirrer at a stirring rate of 320 RPM to avoid agglomeration of polymer particles. After 3 min of stirring, the stirring rate was lowered to 120 RPM and maintained for 24 h, during which the beaker was covered with plastic wrap to prevent air contact. Then, the solution was filtered through a membrane with a pore size of 1.6 μm under 14.7 psia filtration pressure to remove all microgels. The viscosity of the prepared

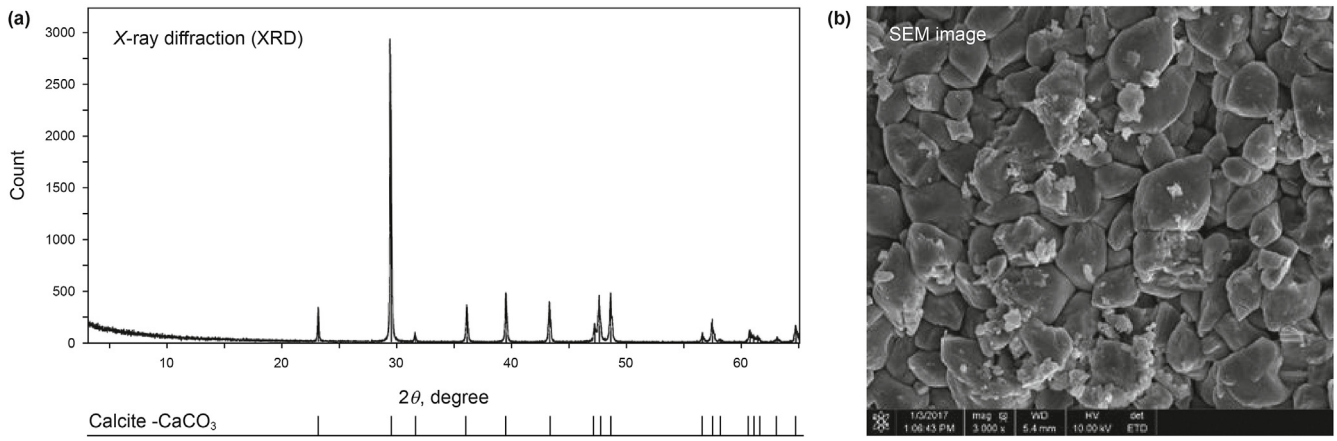

Fig. 1. The results of core analysis (SEM image is reprinted from Lee et al., 2019).

Table 1
Results of XRF analysis for mineral composition of calcite core.

Mineral composition, %			LOI, %
CaO	MgO	Si	
55.8	0.21	0.19	43.68

Note: LOI (loss on ignition): When a sample is heated to 1,000–1,200 °C until there is no change in mass, volatile or thermally decomposable components in the sample are removed, leaving only incombustibles. LOI is the amount of mass loss expressed as a percentage of the sample.

Table 2
Results of routine core analysis for calcite cores.

Core sample	Pore volume, cm^3	Porosity, %	Permeability, mD
Core-1	40	29	35
Core-2	42	30	36
Core-3	35	25	38
Core-4	45	32	38
Core-5	42	30	37
Core-6	46	33	45
Core-7	46	33	41
Core-8	40	29	46

polymer solution was measured by a viscometer and an ultra-low viscosity adapter, which can measure the viscosity of the solution in the range of 1–10 cP with 1% error.

In order to maximize the displacement efficiency, the mobility ratio needs to be lower than 1, which is based on an examination of the relative permeability ratio and viscosity ratio. According to Wang et al. (2009), when the polymer viscosity is equal to the oil viscosity, the oil displacement efficiency is improved by the reduced mobility ratio. Therefore, in this study, the polymer concentration was chosen to produce a polymer viscosity identical to the 5.75 cP of the oil. Fig. 2 shows the measured viscosity for DSW as a function of the shear rate with various polymer concentrations. The viscosity measurements were repeated three times for all cases to ensure reproducibility. Since the typical shear rate in an oil reservoir is around 8 s^{-1}, i.e., the frontal velocity is 1–2 ft/day (Nilsson and Rothstein, 2015), the polymer concentration was selected at a shear rate of 8 s^{-1}. Consequently, the polymer concentrations in the injected water samples were 2,000, 1,250, and 450 ppm for SW, DSW, and RW, respectively (Table 5). Since the viscosities of the oil and the injected fluid were the same, the mobility ratio can be calculated as the ratio of the water relative permeability at residual oil saturation to the oil relative permeability at connate water saturation and expressed as follows (Fanchi, 2010):

Table 3
Chemo-physical properties of crude oil.

API gravity, °	Specific gravity	Viscosity at 60 °C, cP	Acid number, mg KOH/g	Base number, mg KOH/g
32.7	0.861	5.75	0.1	1.1

Table 4
Characteristics of formation water and injection water.

Water		Composition, ppm					TDS	pH
		Ca^{2+}	Mg^{2+}	Na^{+}	Cl^{-}	SO_4^{2-}		
Formation water		12,778	1,377	44,726	90,872	202	150,000	3
Injection water	SW	423	1,352	10,763	19,462	**3,000**	**35,000**	7
	DSW	60	193	1,538	2,709	**500**	**5,000**	7
	RW	13	4	30	5	**10**	**120**	7

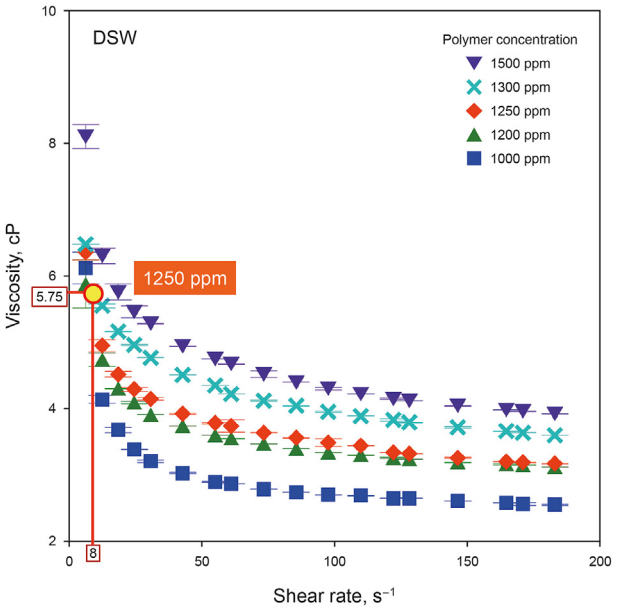

Fig. 2. Viscosity analysis of polymer solution to determine polymer concentration.

Table 5
Determined polymer concentrations and initial mobility ratios.

Injection water	Polymer concentration, ppm	Mobility ratio *M*
SW	2,000	0.54
DSW	1,250	0.62
RW	450	0.41

$$M = \frac{K_{rw}/\mu_w}{K_{ro}/\mu_o} = \frac{K_{rw}\mu_o}{K_{ro}\mu_w} = \frac{K_{rw}}{K_{ro}} \quad (1)$$

where K_{rw} is the relative permeability of water; K_{ro} is the relative permeability of oil; μ_w is the water viscosity, cP; μ_o is the oil viscosity, cP.

Based on the above equation, the calculated mobility ratios were 0.54, 0.62, and 0.41 for SW, DSW, and RW, which are lower than 1.

2.3. Experimental methods

In this section, the experimental procedure used in this study is reviewed, including the coreflooding, spectrophotometry for effluent analysis, and contact angle measurement.

2.3.1. Coreflooding

The experimental system is illustrated in Fig. 3. The aged carbonate core was placed in a core holder with confining pressure of 1,600 psia and system temperature of 60 °C maintained by an electrical heating jacket. During the experiments, in order to assess the effects of the low-salinity water injection method (secondary recovery process) and low-salinity polymer injection method (tertiary recovery process), 3 pore volumes (PV) of the former and 4 PV of the latter were continuously injected. In both stages, fluid was injected at a constant rate of 0.1 mL/min, corresponding to a frontal velocity of 1–2 ft/day, to ensure proper chemical reaction with a minimized capillary end effect (Salih et al., 2016). During the coreflooding experiments, the pressure difference between the inlet and the outlet was measured to estimate polymer retention. In addition, the oil and brine saturations were measured to calculate the relative permeability for the entire core.

2.3.2. Spectrophotometry

In order to quantitatively analyze the amount of adsorbed polymer, the produced polymer mass in the effluents was measured with an ultraviolet-visible (UV-Vis) spectrophotometer. For the measurement, 2 mL of the effluent were mixed with 2 mL of 5 mol/L acetic acid in a conical tube. After the solution was stirred for 4 h, 2 mL of 5% sodium hypochlorite were added and stirred for 5 min. The UV-Vis absorbance was measured at wavelengths of 470 and 520 nm to estimate the polymer concentration in the fluid samples. Before measuring the absorbance of the effluents, the absorbance for the reference solutions was measured to produce a calibration curve. A linear relationship of absorbance with polymer concentration was obtained using polymer solutions with concentrations of 0, 500, 1,000, 1,500, 2,000, and 2,500 ppm. Based on the calibration curve, the absorbance of the effluent was measured to estimate the relative polymer mass. The absorbance was measured three times to ensure reproducibility.

2.3.3. Contact angle

In order to evaluate the wettability alteration phenomena during the LSPF process, the contact angle was measured before and after LSPF. This analysis used the captive droplet method proposed by Yousef et al. (2011). The core was cleaned using a laboratory non-contaminated wiper to remove the extra fluids on the surface and was polished with six different grades of sandpaper to minimize the roughness effect, as suggested by AlShaikh and Mahadevan (2016) and Yousef et al. (2011). The cleaned core was submersed in formation water or injection water for 1 h to achieve chemical equilibrium. The moment at which a 10 μL oil droplet formed on the rock surface was captured by a digital camera for low-bond axisymmetric drop shape analysis (Stalder et al., 2010). The measurement process was repeated three times at room temperature (25 °C).

3. Results and discussion

3.1. Effect of salinity of injection water

In this section, the effects of salinity of injection water on polymer efficiency were analyzed when LSPF is adopted in acidic carbonate reservoirs. The polymer retention and wettability alteration during LSPF in acidic carbonate reservoirs were measured at least three times to ensure reproducibility. The final EOR also was investigated after both LSWF and LSPF. The injection fluid for the experiments was prepared by mixing polymer with low-salinity water of three different water types, i.e., SW, DSW, and RW.

3.1.1. Polymer retention

Before coreflooding experiments, the zeta potential of the polymer solution was measured to evaluate its stability, which is related to polymer degradation and adsorption. The zeta potential is the electrokinetic potential difference between rock–brine interfaces and is commonly used as a key indicator for stability of colloidal dispersions. The zeta potential of the polymer solution made with SW, DSW, and RW was determined through the laser doppler electrophoretic light scattering method, which measures the electrophoretic mobility of molecules and particles in solution. Based on the literature (Brandrup et al., 2005; Zhang et al., 2011), the optimal values of the refractive index and dielectric constant for the polymer solutions were 1.35 and 1.82, respectively, which were used for the analysis herein. Fig. 4 shows the intensity as a function of zeta potential for the polymer solutions mixed with different water types. The zeta potential is a function of the sign and

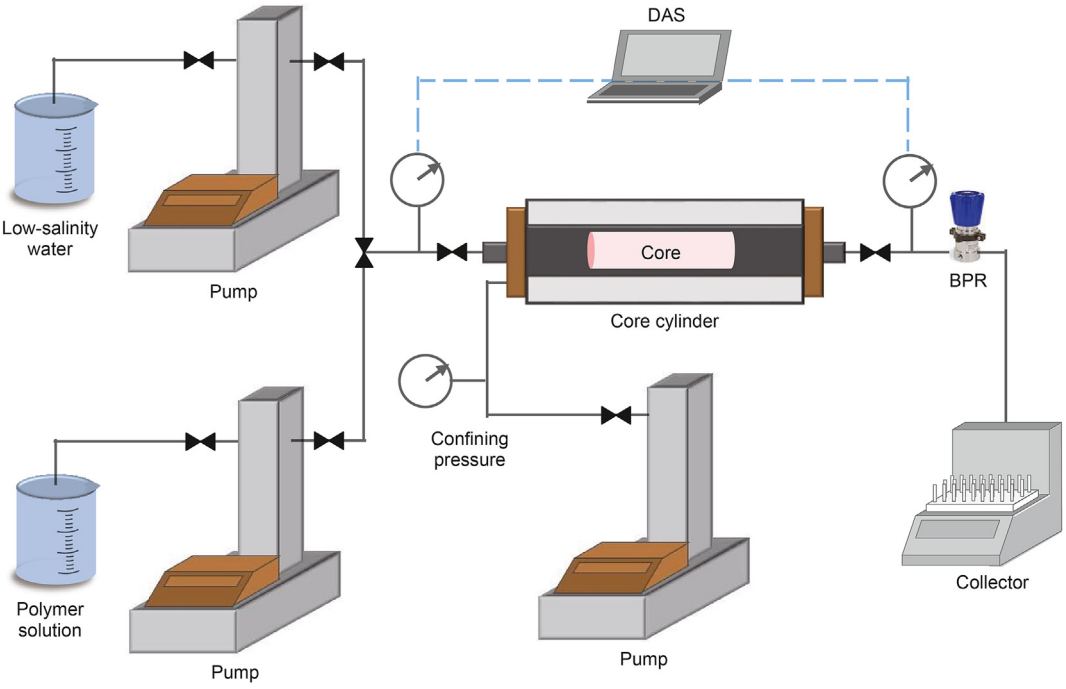

Fig. 3. Diagram of the LSPF experimental system.

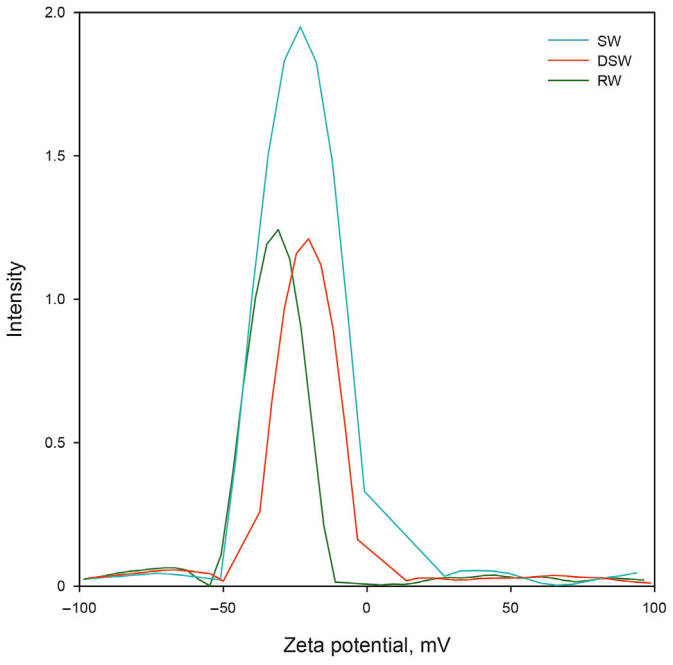

Fig. 4. The measured zeta potential of the polymer solutions mixed with different water types.

magnitude of the electric surface charges between two phases. The magnitude indicates the degree of electrostatic repulsion between adjacent and similarly charged particles (Hanaor et al., 2012). For example, a high zeta potential indicates stability of the fluid, i.e., the solution will resist aggregation. On the other hand, when the potential is small, attractive forces exceed this repulsion and the particles may flocculate. The results showed that the maximum intensity values for SW and DSW were obtained at zeta potentials of 22.50 and 21.13 mV, respectively, while the highest intensity value for RW was detected at 31.85 mV. Therefore, RW was expected to yield the lowest polymer adsorption as it was more stable than the others.

When low-salinity water-based polymer solution is injected into carbonate rock, the chemical reaction between water—oil—rock causes polymer degradation and adsorption, leading to viscosity reduction of the injected polymer solution (Zhang and Seright, 2013). The polymer adsorption induces permeability reduction, which yields an increase in pressure difference between the inlet and outlet during flooding. During LSPF, the pressure difference (ΔP) between the ends of the core was monitored to determine the mobility and permeability reduction caused by polymer adsorption. Using the measured ΔP, polymer retention parameters were determined as proposed by Zaitoun and Chauveteau (1998), including the mobility reduction factor (R_m) and permeability reduction factor (R_k, also named residual resistance factor) (Table 6). The former is the ratio of the pressure difference during LSWF to that of LSPF. A large R_m value indicates a significant pressure difference during LSPF compared to that of LSWF, signifying a large mobility reduction. In the same manner, larger R_k means greater permeability reduction in LSPF than in LSWF. According to AlSofi et al. (2018), these parameters can be used reliably to evaluate the permeability reduction due to polymer degradation and adsorption.

The mobility reduction factor and permeability reduction factor can be calculated from the following equations (Zaitoun and Chauveteau, 1998; AlSofi et al., 2018; Chauveteau et al., 2002):

$$R_m = \frac{\Delta P_{LSPF}}{\Delta P_{LSWF}} \tag{2}$$

$$R_k = \frac{\Delta P_{LWALP}}{\Delta P_{LSWF}} \tag{3}$$

where ΔP_{LSWF} is the pressure difference during LSWF, psi; ΔP_{LSPF} is the pressure difference during LSPF, psi; ΔP_{LWALP} is the pressure difference during LSWF followed by LSPF, psi.

Table 6
The estimated polymer retention parameters.

Injection water	Mobility reduction factor R_m	Permeability reduction factor R_k
SW	3.7	2.0
DSW	1.6	1.1
RW	4.9	3.2

Fig. 5 shows ΔP as a function of pore volume injected (PVI) for each injection water. The blue, red and green curves indicate the pressure difference of SW, DSW, and RW, respectively. Trend curves for ΔP are illustrated in white. After LSWF is complete (3 PV), ΔP increases sharply due to injection of high-viscosity polymer solution as the LSPF stage begins. When ΔP was stable during LSPF, the calculated R_m values were 3.7 and 1.6 for SW and DSW, respectively. In other words, the mobility decrement of DSW was less than that of SW due to its lower salinity. When RW was selected for the injection fluid, the value of R_m was the highest, despite it having the lowest salinity. According to Chauveteau et al. (2002), the mobility reduction ratio defined by R_m strongly depends on polymer adsorption.

On the other hand, since polymer adsorption may reduce the effective permeability, the permeability reduction factor R_k can be a useful indicator to determine the effect of polymer adsorption. Here, R_k was determined as the ratio of permeability before to permeability after LSPF. Since the permeability pre-LSPF was measured after LSWF, the permeability post-LSPF was obtained when pressure stabilized during the additional low-salinity waterflooding after LSPF (LWALP) to minimize the experimental error (Park et al., 2015). After LWALP, it was assumed that the entrapped polymer solution was completely removed, and that the measured permeability reduction was only induced by the polymer adsorption. As listed in Table 6, the R_k value for SW was 2.0, which was 1.8 times greater than the 1.1 of DSW. The higher R_k value signifies greater permeability reduction due to polymer adsorption. In other words, the polymer adsorption magnitude for DSW was smaller than that of SW, primarily due to its lower salinity. In the high-salinity condition, which implies strong ionic strength, polymer molecules cannot maintain their structure, and thus, the bonds within the polymer chains are disrupted, leading to aggregation of polymer molecules (Yoo and Lee, 2020). Therefore, decreasing the salinity can prevent the charge screening effect, which strongly depends on polymer stability. Meanwhile, although the salinity of RW was lowest, the R_k was largest, at 3.2, implying that the permeability after LSPF was reduced by about one-third compared to the value before LSPF. It also indicates that polymer adsorption was greatest for RW, likely due to its lowest SO_4^{2-} content, which can affect polymer stability. A more detailed analysis of the SO_4^{2-} ion effects on polymer adsorption onto rock grain surfaces is provided in Section 3.2.

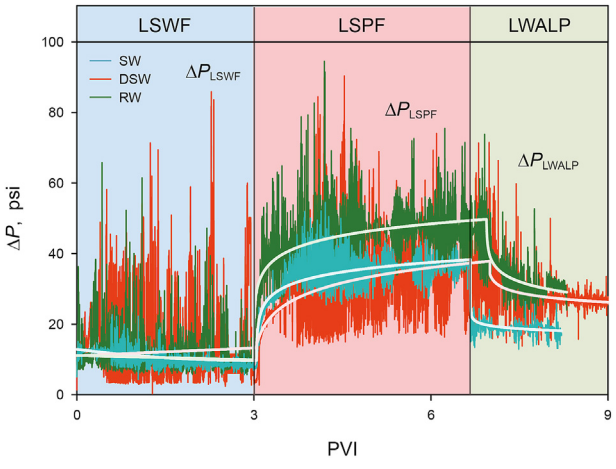

Fig. 5. The measured pressure difference during coreflooding experiments.

Polymer retention occurs when the polymer solution propagates through the core. The magnitude of the phenomenon can be directly determined by effluent analysis, which measures the amount of drained polymer. This study adopted the UV-Vis spectrophotometer for this analysis. In order to analyze the effect of reservoir formation water pH, effluent analysis was performed after LSPF with DSW for reservoirs saturated with acidic or neutral formation water (Fig. 6a). After LSPF was completed at the injection of 4 PV, 44.6% polymer mass ($A = (m_{injected} - m_{produced})/m_{injected}$) was adsorbed in the acidic reservoir condition, while 39.1% (B) of the polymer remained in the core due to adsorption in the neutral reservoir condition. Therefore, the magnitude of polymer adsorption in the acidic condition is larger than that of the neutral condition, indicating lower efficiency of injected polymer when the reservoir contains acidic formation water.

The polymer adsorption phenomenon in the acidic condition was analyzed in detail for each water type: SW, DSW, and RW. Fig. 6b illustrates the ratio of adsorbed polymer to injected polymer in an acidic reservoir condition for different water types. For SW, 51.9% of the injected polymer remained in the core due to adsorption, while 44.6% and 53.8% were retained in the rock for DSW and RW, respectively. In comparison to the results from the SW injection, the magnitude of polymer adsorption was smaller in DSW and larger in RW. Accordingly, consistent results were observed for R_k, i.e., greater permeability reduction was detected with larger amount of polymer adsorbed. The results of the coreflooding tests and spectrophotometer measurements show different trends from the results of zeta potential measurements performed before the injection. Although RW was the most stable under static conditions at room temperature and pressure, however, because of low salinity and low SO_4^{2-} concentration in RW, the polymer might be more affected by the reservoir conditions. In other words, when low-salinity polymer solution with low SO_4^{2-} concentration related to polymer stability was injected into an acidic carbonate reservoir, the polymer adsorption can be aggravated. Therefore, injecting DSW with low salinity (5,000 ppm) and 500 ppm SO_4^{2-} ions yields the minimum polymer adsorption and permeability reduction.

3.1.2. Wettability alteration

Before injecting the synthetic fluids, the zeta potential was measured to evaluate the possible rock wettability. The measurements were performed on both rock–brine (RB) and rock–oil–brine (ROB) systems equilibrated with formation water and injection water (SW, DSW, and RW). Solutions were prepared in a conical tube consisting of 50 mL each of formation water and injection water; 0.2 g of rock powder was added to the solution and was mixed using an ultrasonicator at 60 °C (AlSofi et al., 2019). The zeta potential of the supernatant was measured three times. As shown in Fig. 7, when the rock particles equilibrated in formation

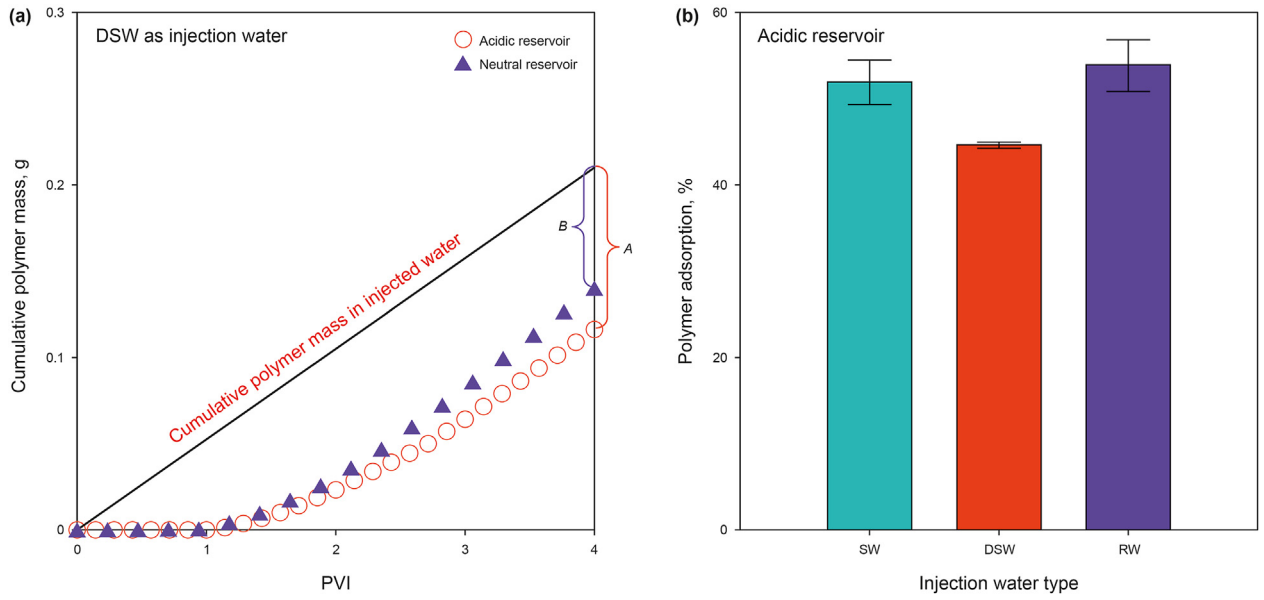

Fig. 6. The results of effluent analysis. (**a**) Cumulative polymer mass with DSW injection; (**b**) Polymer adsorption by injection water type.

water, the zeta potential values were positive for both RB and ROB systems. On the other hand, the zeta potential values were negative for all injection water types in both systems. This implies that the initial reservoir condition is more likely to be an oil-wet state, but that the injection of the three types of brines has the potential to alter the wettability to a water-wet state. In addition, the larger absolute value indicates the greater potential of the wettability alteration. The measured zeta potential for RW was −20.8 mV in the RB system and −35.7 mV in the ROB system, while those for SW and DSW were −5.2 and −8.0 mV in the RB system and −7.9 and −15.0 mV in the ROB system, respectively. Therefore, according to the measured zeta potential values, it was expected that RW would be the most effective injection water for LSPF in terms of wettability alteration.

Wettability alteration is one of the major machanisms of LSPF that contributes to oil recovery enhancement in carbonate reservoirs. When the wettability of carbonate rock changes from oil-wet to water-wet, it improves the mobility of the oil phase, and more oil is produced. To closely investigate the wettability before and after LSPF, the relative permeabiltiy was measured and correlated by the

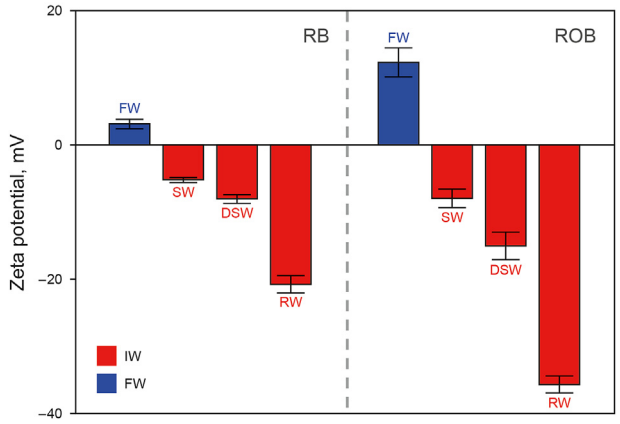

Fig. 7. The measured zeta potential of formation water (FW) and injection water (IW) in rock–brine (RB) and rock–oil–brine (ROB) systems.

Pirson's correlation for both acidic and neutral reservoir conditions (Pirson, 1958; Ahmed, 2010). Fig. 8 shows the relative permeability curves before and after LSPF using the three types of injection fluids in the acidic reservoir. For all types of water, it was observed that the saturation values of the cross points were shifted right after LSPF. This means that the wettability was altered to a water-wet state by injection of low-salinity polymer solution. In terms of ΔS_{or} ($\Delta S_{or} = S_{or,before} - S_{or,after}$), which denotes the change in residual oil saturation ($S_{or} = 1 - S_{wmax}$) before and after LSPF, the saturation decreased from 29.40% (100%–71.60%) to 12.02% (100%–87.98%), a decrease of 17.38%, when DSW was injected in the acidic reservoir condition. Meanwhile, when the formation water was neutral, ΔS_{or} was 14.8%. Therefore, the increment of wettability alteration to water-wet was greater in the acidic reservoir than in the neutral reservoir. When the high-salinity SW was injected as shown in the left panel of Fig. 8, ΔS_{or} was 14.92% and smaller than that of DSW (17.38%), which indicates smaller wettability alteration for SW compared to DSW. This can be explained mainly by addition of polymer, as the water type was unchanged in LSWF and LSPF for each experimental case. The negatively charged polymer molecules might directly affect the wettability alteration or help SO_4^{2-} ions to reduce the surface potential of rock, allowing Ca^{2+} and Mg^{2+} ions to detach oil from the rock surface. When the salinity is high, the polymer structure is degraded and the activity of SO_4^{2-} ion is hindered, resulting in less wettability alteration. On the other hand, ΔS_{or} was smallest at 9.97% with RW, as was the wettability alteration magnitude, despite having the lowest salinity. This is because RW contains the lowest concentration of SO_4^{2-} ions. Therefore, SO_4^{2-} and polymer are important factors of wettability during LSPF in acidic carbonate reservoirs.

According to Afekare and Radonjic (2017), AlShaikh and Mahadevan (2016), and Derkani et al. (2018), the contact angle is an excellent indicator of the wettability between rock and fluid. In order to evaluate wettability alteration during LSPF, the contact angle was measured before and after LSPF in both acidic and neutral conditions. In this study, the cores were polished with sandpaper to minimize the roughness effect, and it was assumed that the effect of surface roughness was negligible. Fig. 9 shows the contact angle change before and after LSPF in the acidic reservoir for each water type. It was found that the observed wettability

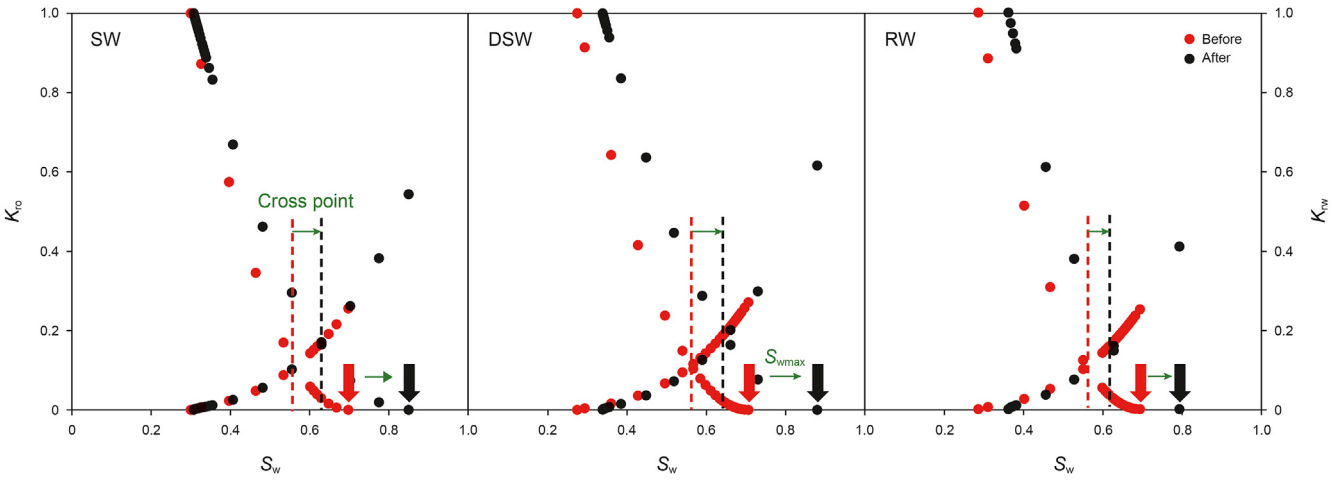

Fig. 8. The changes in relative permeability curves by water type in an acidic reservoir.

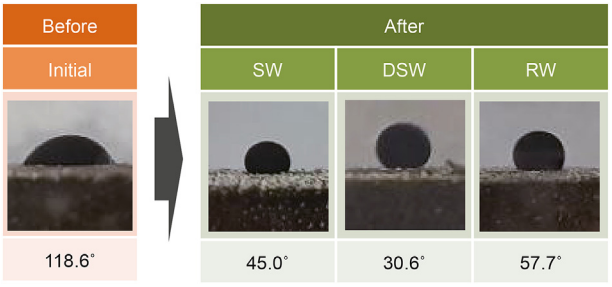

Fig. 9. Contact angle measurements in a carbonate core containing acidic water.

alterations corresponded well with the results of the relative permeability analysis. In the initial state, the contact angle at the rock surface was 118.6°, implying that the rock surface is in an oil-wet state. This is because the carboxyl group of the oil was directly adsorbed on the surface of the carbonate rock during the aging process. After LSPF was complete, the contact angles decreased significantly and the wettability was altered to a water-wet state for all water types. When low-salinity polymer solution was injected, SO_4^{2-} ions in the injected fluid adsorbed to the rock surface and lowered the surface potential. Then, divalent cations such as Ca^{2+} and Mg^{2+} can easily access the rock surface and detach the oil from the surface. Since the polymer molecules are negatively charged, they can directly adsorb on the rock surface or help SO_4^{2-} ions to decrease the surface potential. For example, the contact angle after LSPF with DSW was 30.6°, which is lower than the 45.0° and 57.7° for SW and RW, respectively. This indicates that DSW had a sufficiently low TDS and contained sufficient SO_4^{2-} ions and polymer molecules. On the other hand, SW contained the highest concentrations of SO_4^{2-} and polymer molecules; however, due to its highest salinity, it might be difficult to lower the surface potential or to allow divalent cations to access the rock surface. With RW, although its salinity was the lowest, the surface potential might not be reduced sufficiently as the fluid did not contain enough SO_4^{2-} ions and polymer molecules. Therefore, DSW was the most effective injection fluid in terms of wettability alteration during the LSPF process.

3.1.3. EOR efficiency

The previous section reported that polymer adsorption and wettability alteration were greatly influenced by LSPF. Moreover, the magnitude of the change before and after flooding was larger for the acidic reservoir than for the neutral reservoir. Therefore, in this section, the enhanced oil volumes achieved by the LSPF process for acidic and neutral reservoirs were analyzed by quantifying the EOR. The EOR value was calculated using the recovery factor before and after LSPF when no more oil was produced. As can be seen in Fig. 10a, when DSW was selected as the injection fluid, the EOR by LSPF was enhanced by 17.9% for the neutral reservoir, while that for the acidic reservoir was increased by 23.9%. This is because, for the acidic carbonate reservoir, the effect of the polymer on wettability alteration was greater than that of polymer adsorption by acidic formation water. Consequently, the LSPF process in the carbonate reservoir was more efficient in acidic formation water than in the neutral condition.

In particular, EOR values for the acidic reservoir over three types of water with different salinity levels (SW, DSW, and RW) are shown in Fig. 10b. When RW with the lowest salinity was injected for LSPF, the EOR was 15.6%, which was lower than those of DSW and SW. Therefore, RW is not always desirable for LSPF although its salinity level is the lowest. However, when DSW was selected as the injection fluid, the EOR was 23.9% and was higher than that of SW (21.3%). This is because the higher salinity level of SW caused greater polymer adsorption and less wettability alteration than in the DSW case. The difference in EOR for the three water types may be caused by the concentration of the SO_4^{2-} ions, which prevents polymer adsorption and facilitates wettability alteration, resulting in oil detachment from the rock grains. Since RW did not contain a sufficient amount of SO_4^{2-} ions, the final EOR value was not efficiently increased, although its salinity was lower than those of the other two water types. In the same manner, despite having a higher salinity than RW (TDS 120 ppm, SO_4^{2-} 10 ppm), selecting DSW (TDS 5,000 ppm, SO_4^{2-} 500 ppm) yielded the highest recovery (23.9%) among the used water types in this study due to its sufficient SO_4^{2-} content. Additionally, a larger amount of oil was produced using 62.5% of the polymer in DSW (polymer 1,250 ppm) compared to SW (polymer 2,000 ppm). It indicates that polymer efficiency was also the highest in DSW.

3.2. Effect of SO_4^{2-} concentration in injection water

In Section 3.1, the effect of injection water salinity was closely investigated. The results showed that oil recovery was enhanced by a low salinity of the injection fluid; however, it was also expected that the SO_4^{2-} concentration should be sufficient in the injected

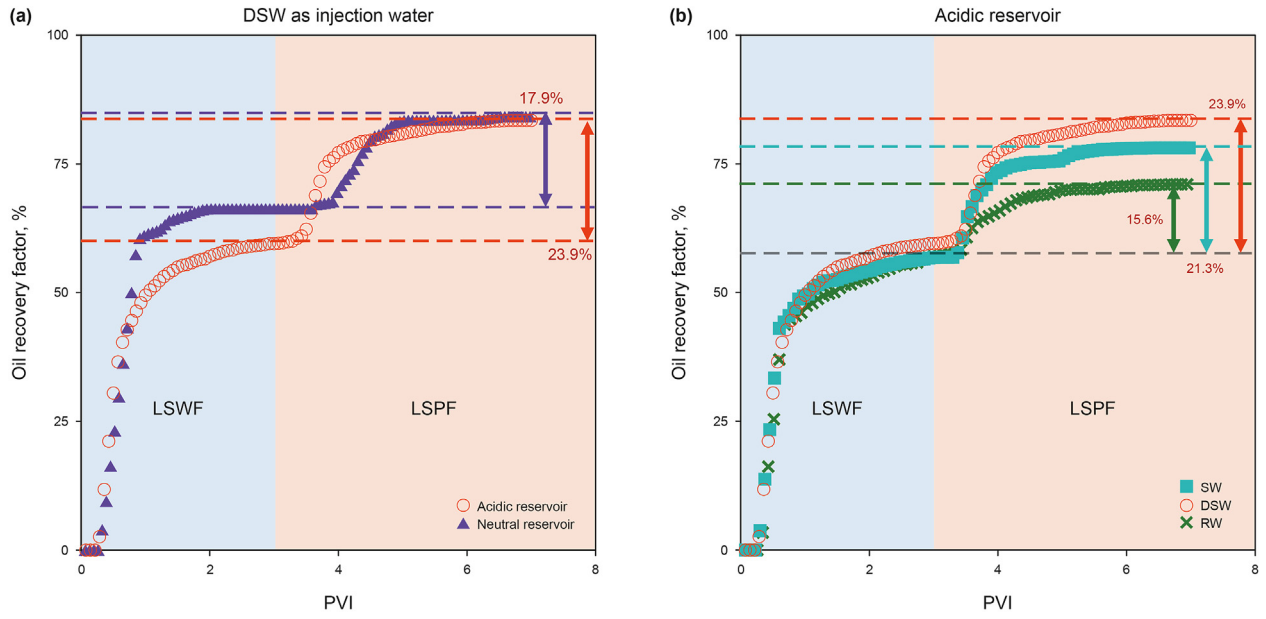

Fig. 10. The measured oil recovery.

fluid. According to the results of coreflooding experiments performed by Lee et al. (2019), a high concentration of SO_4^{2-} ions in the injection water improved oil recovery in a carbonate reservoir containing neutral formation water. Safavi et al. (2020) observed that the optimal range of SO_4^{2-} concentration for neutral dolomite reservoirs was between 5.227 and 0.875 percentages. Song et al. (2020) reported that a higher SO_4^{2-} concentration does not always result in a higher oil recovery. Therefore, in this section, more detailed analysis was performed, focusing on the SO_4^{2-}concentration. For both acidic and neutral reservoir conditions, injection fluids with different concentrations of SO_4^{2-} ions (500, 1,000, 2,000, and 3,000 ppm) and the same TDS were prepared. These synthetic fluids were injected to investigate the polymer efficiency in terms of polymer adsorption, wettability alteration, and oil recovery.

Fig. 11 shows the result of effluent analysis for the acidic condition. The polymer adsorption magnitude was reduced as the concentration of SO_4^{2-} contained in the injection fluid was high.

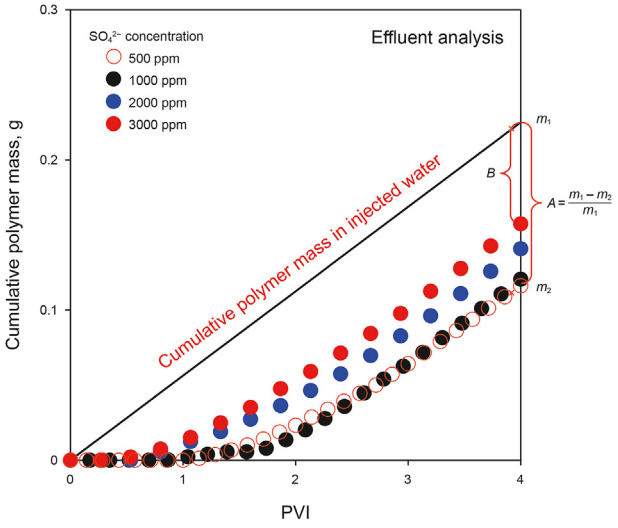

Fig. 11. The result of effluent analysis in an acidic reservoir condition.

When the SO_4^{2-} concentration was 500 ppm in DSW, 44.6% ($A = (m_1 - m_2)/m_1$) of the injected polymer was adsorbed, while that at a concentration of 3,000 ppm was 31.5% (B). This is mainly because both the SO_4^{2-} ion and the polymer molecule are negatively charged. Consequently, the repulsive interactions may maintain the structure of the polymer chains. Accordingly, at a higher ion concentration, the polymer stability is improved, which interferes with the adsorption of the polymer molecules on the grain surface. The comparison with 3,000 ppm SO_4^{2-} indicates that the effect was greater in the acidic reservoir condition than in the neutral condition. Therefore, in terms of polymer adsorption in the acid reservoir, DSW with 3,000 ppm SO_4^{2-} ions was the most efficient injection fluid.

The wettability alteration was measured by relative permeability and contact angle change for both acidic and neutral reservoir conditions. In Fig. 12, the change in relative permeability curves before and after LSPF is illustrated when DSW with 500 ppm and 3,000 ppm SO_4^{2-} was injected in the acidic reservoir. The intersection of K_{ro}–K_{rw} curves shifted more to the right for the higher SO_4^{2-} concentration (3,000 ppm; red dashed line) than in the lower concentration (500 ppm; black dashed line). This indicates that the wettability was altered to a more water-wet state with higher SO_4^{2-} concentration in the injection water. Since the SO_4^{2-} ion reduces the surface potential of rock, the oil attached on the carbonate rock surface induces an oil-wet state and can be detached from the rock surface. In addition, the polymer molecule can contribute to the role of SO_4^{2-} ions. Therefore, a higher concentration of SO_4^{2-} detaches more oil, altering the wettability to a greater water-wet state. After LSPF, the residual oil saturation ($S_{or} = 1 - S_{wmax}$) for the 3,000 ppm case was 6.26% (100% – 93.74%), while that of the 500 ppm case was 12.02% (100% – 87.98%). In other words, a higher SO_4^{2-}concentration in the injection water results in greater alteration to the water-wet state, leading to less residual oil in the core. Therefore, in this study, the injection of DSW containing 3,000 ppm of SO_4^{2-} ions altered the best wettability.

Based on the analyses above, the produced oil was measured during injection in both acidic and neutral reservoir conditions. The oil recoveries for the acidic reservoir are shown in Fig. 13. After LSWF (3 PVI injection), a larger amount of oil was produced with higher concentration of SO_4^{2-} ions. This is because SO_4^{2-} allows the

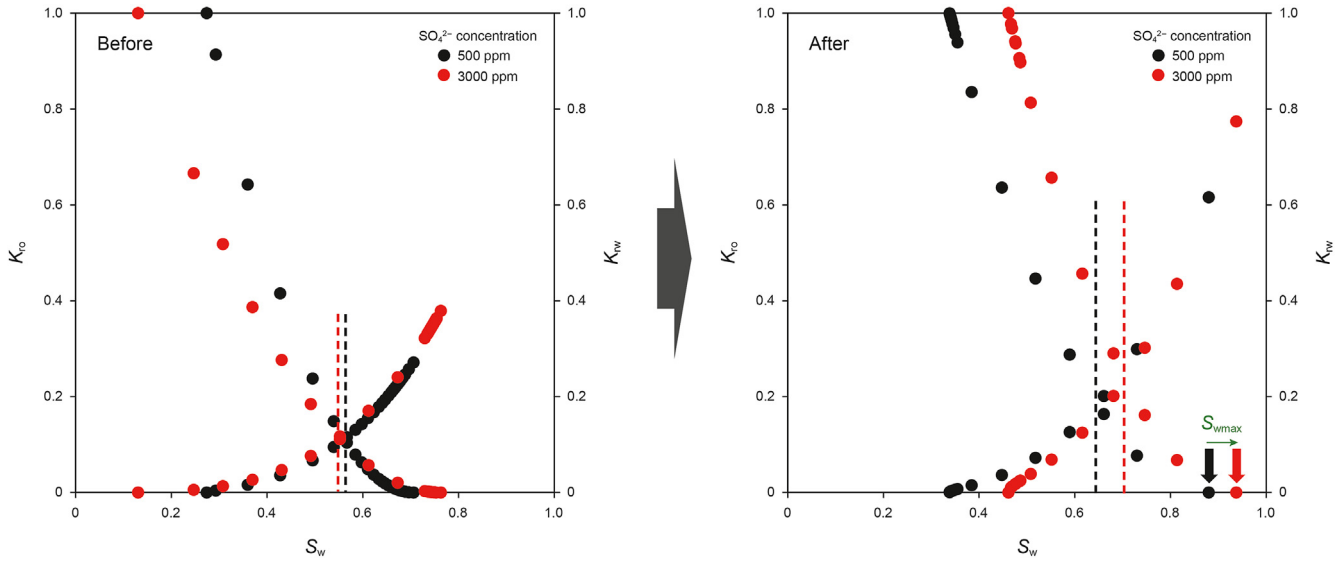

Fig. 12. The changes in relative permeability curves for the acidic reservoir condition.

oil to detach from the grain surface, altering the wettability of the surface. After the total flooding period (LSWF and LSPF) (7 PVI), the final oil recovery factor ranged from 83.44% to 92.80% in the range of 500 to 3,000 ppm SO_4^{2-}. The increased SO_4^{2-} concentration prevented polymer adsorption and facilitated wettability alteration with the help of polymer molecules, resulting in high oil recovery. When the oil recovery after LSWF for DSW was based, the EOR efficiency was 23.93% for DSW and 33.29% for DSW containing 3,000 ppm SO_4^{2-}. This indicates that a larger amount of oil can be produced with the same polymer concentration by adjusting the SO_4^{2-} concentration in the injection fluid. In other words, the SO_4^{2-} ion plays an important role in improving polymer efficiency.

With regard to pH, oil recovery after LSWF was higher in the neutral reservoir than in the acidic reservoir. The SO_4^{2-} ion without polymer was more effective in the neutral condition. After the LSPF process with 500 ppm of SO_4^{2-}, oil recovery was slightly higher in the neutral condition, although the difference was not significant. When the concentration was high at 3,000 ppm, however, oil recovery was higher in the acidic condition than in the neutral condition. The recovery factors after total flooding in the acidic reservoir were 83.4% and 92.8% for SO_4^{2-} concentrations of 500 and 3,000 ppm, respectively. Those in the neutral reservoir did not show a large difference when the SO_4^{2-} concentration increased from 500 to 3,000 ppm. This is because the effect of the SO_4^{2-} ion, which yielded lower polymer adsorption and greater wettability alteration, was greater in the acidic reservoir. The polymer efficiency improved by addition of SO_4^{2-} in both pH conditions. When the reservoir was neutral, the increment of oil recovery per 1 g of polymer was 0.78% and 1.05% for 500 and 3,000 ppm SO_4^{2-}, respectively. On the other hand, in the acidic reservoir condition, 1 g

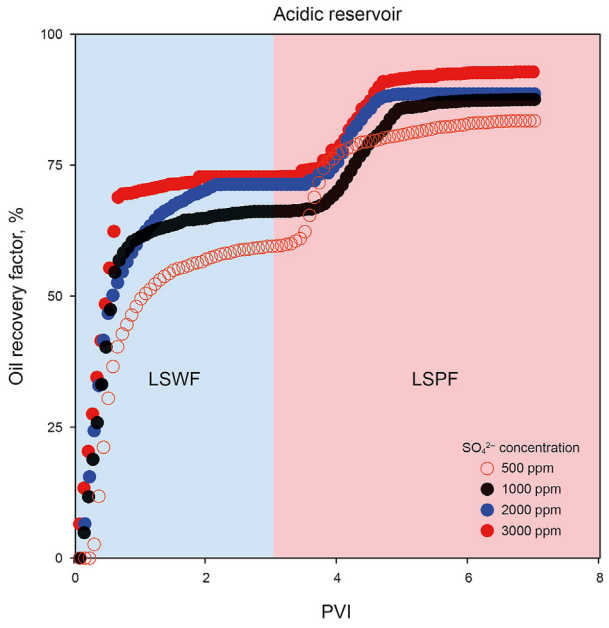

Reservoir	Acid		Neutral	
SO_4^{2-} concentration, ppm	500	3000	500	3000
Recovery factor (after LSWF), %	59.51	72.75	66.26	76.47
Recovery factor (after LSPF), %	83.44	92.80	84.18	85.83

Fig. 13. The measured oil recovery by the injection water containing different SO_4^{2-} concentrations for acidic and neutral reservoir conditions.

of polymer can enhance oil recovery by 1.14%–1.45% for SO_4^{2-} concentrations of 500 and 3,000 ppm, respectively. Therefore, when low-salinity water interacts with a high concentration of SO_4^{2-} ions, LSPF is a more reliable EOR method in an acidic carbonate reservoir than in a neutral reservoir.

4. Conclusions

Since the polymer efficiency can be severely deteriorated in a carbonate reservoir containing "acidic" formation water, the applicability of LSPF for acidic conditions was evaluated. In addition, to design the optimal injection water for the LSPF process, a set of coreflooding experiments was performed for different salinity levels and SO_4^{2-} concentrations, which would be commonly available in the field.

A comparison study showed that the magnitude of the polymer adsorption in the acidic condition is greater than that in the neutral condition. This indicates that the efficiency of the injected polymer is lower when the reservoir contains acidic formation water. In terms of wettability alteration, the degree of wettability alteration to water-wet was greater in the acidic reservoir than in the neutral reservoir. With regard to pH condition, it was found that the use of polymer in an acidic reservoir was not as efficient as in a neutral reservoir.

From the results of salinity effect with three types of injection water, lowering the salinity of SW can improve polymer stability, resulting in lower polymer adsorption and greater wettability alteration, as shown in the DSW case. However, for RW, polymer adsorption was greater and wettability alteration was lower than for the other water types despite having the lowest salinity. This is because RW contains the lowest concentration of SO_4^{2-}. Therefore, DSW (TDS 5,000 ppm and SO_4^{2-} 500 ppm) yielded the highest recovery (23.9%) among the water types.

The detailed analysis focused on SO_4^{2-} concentration. The SO_4^{2-} ion improved polymer stability by maintaining the structure of the polymer chains, and the polymer molecule helped the SO_4^{2-} ion to reduce the surface potential of the rock, allowing the oil to detach from the rock surface. When the concentration of SO_4^{2-} ions in the injected fluid was high, its interaction with the polymer molecule prevented polymer adsorption and facilitated wettability alteration, resulting in high oil recovery. In other words, a larger amount of oil can be produced with the same polymer concentration by adjusting the SO_4^{2-} concentration.

Consequently, even though the reservoir was acidic, the LSPF process was as efficient as in a neutral reservoir when low-salinity injection water contained a high concentration of SO_4^{2-} ions. Therefore, when designing RW as injection water for an acidic reservoir, the LSPF method proposed in this study would be a reliable method if the optimal SO_4^{2-} concentration is used. In addition, the proposed LSPF method is more environmentally friendly as it requires a smaller amount of polymer.

Declaration of competing interest

The authors declare that they have no known competing financial interests or personal relationships that could have appeared to influence the work reported in this paper.

Acknowledgements

This work was supported by the Energy Efficiency & Resources (No. 20212010200010) and the "Development of Intelligential Diagnosis, Abandonment Process and Management Technology for Decrepit Oil and Gas Wells" (No. 20216110100010) of the Korea Institute of Energy Technology Evaluation and Planning (KETEP) grant funded by the Korean Government Ministry of Trade, Industry & Energy.

References

Afekare, D.A., Radonjic, M., 2017. From mineral surfaces and coreflood experiments to reservoir implementations: comprehensive review of low-salinity water flooding (LSWF). Energy Fuel. 31 (12), 13043–13062. https://doi.org/10.1021/acs.energyfuels.7b02730.

Ahmed, T., 2010. Chapter 5 - Relative permeability concepts. In: Reservoir Engineering Handbook, fourth ed. Gulf Professional Publishing, Boston.

Al-Anazi, H.A., Sharma, M.M., 2002. Use of a pH sensitive polymer for conformance control. In: International Symposium and Exhibition on Formation Damage Control. Society of Petroleum Engineers. https://doi.org/10.2118/73782-MS.

AlShaikh, M., Mahadevan, J., 2016. Impact of brine composition on calcite wettability: a sensitivity study. SPE J. 21 (4), 1214–1226. https://doi.org/10.2118/172187-PA.

AlSofi, A.M., Wang, J., Kaidar, Z.F., 2018. Smartwater synergy with chemical EOR: effects on polymer injectivity, retention and acceleration. J. Pet. Sci. Eng. 166, 274–282. https://doi.org/10.1016/j.petrol.2018.02.036.

AlSofi, A.M., Wang, J., AlBoqmi, A.M., AlOtaibi, M.B., Ayirala, S.C., AlYousef, A.A., 2019. Smartwater synergy with chemical enhanced oil recovery: polymer effects on smartwater. SPE Reservoir Eval. Eng. 22 (1), 61–77. https://doi.org/10.2118/184163-PA.

Behling, R., Renton, J., Hemler, D., 2002. Geoscience Education in the Mountain State: CATS Earth Science Connections IV Environmental Geochemistry Telecourse. West Virginia Geological & Economic Survey. http://www.wvgs.wvnet.edu/www/geoeduc/es020423.htm.

Bella, F., Porcarelli, L., Mantione, D., Gerbaldi, C., Barolo, C., Gratzel, M., Mecerreyes, D., 2020. A water-based and metal-free dye solar cell exceeding 7% efficiency using a cationic poly (3,4-ethylenedioxythiophene) derivative. Chem. Sci. 11, 1485–1493. https://doi.org/10.1039/c9sc05596g.

Brandrup, J., Immergut, E.H., Grulke, E.A., Abe, A., Bloch, D.R., 2005. Polymer Handbook, fourth ed. John Wiley & Sons, New York.

Chauveteau, G., Denys, K., Zaitoun, A., 2002. New insight on polymer adsorption under high flow rates. In: SPE/DOE Improved Oil Recovery Symposium. Society of Petroleum Engineers. https://doi.org/10.2118/75183-MS.

Choi, S.K., Sharma, M.M., Bryant, S., Huh, C., 2010. pH-sensitive polymers for novel conformance-control and polymer-flood applications. SPE Reservoir Eval. Eng. 13 (6), 926–939. https://doi.org/10.2118/121686-PA.

Derkani, H.M., Fletcher, J.A., Abdallah, W., Sauerer, B., Anderson, J., Zhang, J.Z., 2018. Low salinity waterflooding in carbonate reservoirs: review of interfacial mechanisms. Colloids Interfaces 2 (2), 20. https://doi.org/10.3390/colloids2020020.

Fanchi, J.R., 2010. Chapter 10 - Rock-Fluid Interactions. Integrated Reservoir Asset Management. Gulf Professional Publishing, Boston, pp. 167–185. https://doi.org/10.1016/B978-0-12-382088-4.00010-4.

Gupta, R., Smith, P.G., Hu, L., Willingham, T.W., Cascio, M.L., Shyeh, J.J., Harris, C.R., 2011. Enhanced waterflood for carbonate reservoirs - impact of injection water composition. In: SPE Middle East Oil and Gas Show and Conference. Society of Petroleum Engineers. https://doi.org/10.2118/142668-MS.

Hager, M.D., Esser, B., Feng, X., Schuhmann, W., Theato, P., Schubert, U.S., 2020. Polymer-based batteries-flexible and thin energy storage systems. Adv. Mater. 32 (39), 2000587. https://doi.org/10.1002/adma.202000587.

Hanaor, D., Michelazzi, M., Leonelli, C., Sorrell, C.C., 2012. The effects of carboxylic acids on the aqueous dispersion and electrophoretic deposition of ZrO_2. J. Eur. Ceram. Soc. 32 (1), 235–244. https://doi.org/10.1016/j.jeurceramsoc.2011.08.015.

Khalil, M., Jan, B.M., Tong, C.W., Berawi, M.A., 2017. Advanced nanomaterials in oil and gas industry: design, application and challenges. Appl. Energy 191, 287–310. https://doi.org/10.1016/j.apenergy.2017.01.074.

Khorsandi, S., Qiao, C., Johns, R.T., 2016. Displacement efficiency for low-salinity polymer flooding including wettability alteration. SPE J. 22 (2), 417–430. https://doi.org/10.2118/179695-PA.

Lee, Y., Lee, W., Jang, Y., Sung, W., 2019. Oil recovery by low-salinity polymer flooding in carbonate oil reservoirs. J. Pet. Sci. Eng. 181, 106211. https://doi.org/10.1016/j.petrol.2019.106211.

Masalmeh, S., AlSumaiti, A., Gaillard, N., Daguerre, F., Skauge, T., Skuage, A., 2019. Extending polymer flooding towards high-temperature and high-salinity carbonate reservoirs. In: Abu Dhabi International Petroleum Exhibition & Conference. Society of Petroleum Engineers. https://doi.org/10.2118/197647-MS.

Nilsson, M.A., Rothstein, J., 2015. Effect of fluid rheology and sandstone permeability on enhanced oil recovery in a microfluidic sandstone device. Appl. Rheol. 25, 25189. https://doi.org/10.3933/applrheol-25-25189.

Park, H., Park, Y., Lee, Y., Sung, W., 2018. Efficiency of enhanced oil recovery by injection of low-salinity water in barium-containing carbonate reservoirs. Petrol. Sci. 15 (4), 772–782. https://doi.org/10.1007/s12182-018-0244-z.

Park, H., Han, J., Sung, W., 2015. Effect of polymer concentration on the polymer adsorption-induced permeability reduction in low permeability reservoirs. Energy 84, 666–671. https://doi.org/10.1016/j.energy.2015.03.028.

Pirson, S.J., 1958. Oil Reservoir Engineering, second ed. McGraw-Hill, New York.

Qian, J., Jin, B., Li, Y., Zhan, X., Hou, Y., Zhang, Q., 2021. Research progress on gel polymer electrolyte for lithium-sulfur batteries. J. Energy Chem. 56, 420–437.

https://doi.org/10.1016/j.jechem.2020.08.026.

Safavi, M.S., Masihi, M., Safekordi, A.A., Ayatollahi, S., Sadeghnejad, S., 2020. Effect of SO_4^{2-} ion exchanges and initial water saturation on low salinity water flooding (LSWF) in the dolomite reservoir rocks. J. Dispersion Sci. Technol. 41 (6), 841–855. https://doi.org/10.1080/01932691.2019.1614026.

Salih, T.A., Sahi, S.H., Hameed, O.K., 2016. Rheological evaluation of polymer (Sav 10) for polymer flooding applications. Iraqi J. Chem. Pet. Eng. 17 (1), 37–46.

Shiran, B.S., Skauge, A., 2013. Enhanced oil recovery (EOR) by combined low salinity water/polymer flooding. Energy Fuel. 27 (3), 1223–1235. https://doi.org/10.1021/ef301538e.

Sheng, J.J., 2011. Chapter 5 - Polymer Flooding, Modern Chemical Enhanced Oil Recovery. Gulf Professional Publishing, Boston, pp. 101–206.

Sheng, J.J., Leonhardt, B., Azri, N., 2015. Status of polymer-flooding technology. J. Can. Pet. Technol. 54 (2), 116–126. https://doi.org/10.2118/174541-PA.

Song, J., Wang, Q., Shaik, I., Puetro, M., Bikkina, P., Aichele, C., Biswal, S.L., Hirasaki, G.J., 2020. Effect of salinity, Mg^{2+} and SO_4^{2-} on "smart water"-induced carbonate wettability alteration in a model oil system. J. Colloid Interface Sci. 563, 145–155. https://doi.org/10.1016/j.jcis.2019.12.040.

Sorbie, K.S., 1991. Polymer-Improved Oil Recovery. Springer, Netherlands.

Stalder, A.F., Melchior, T., Müller, M., Sage, D., Blu, T., Unser, M., 2010. Low-bond axisymmetric drop shape analysis for surface tension and contact angle measurements of sessile drops. Colloid. Surface. 364 (1), 72–81. https://doi.org/10.1016/j.colsurfa.2010.04.040.

Standnes, D.C., Skjevrak, I., 2014. Literature review of implemented polymer field projects. J. Pet. Sci. Eng. 122, 761–775. https://doi.org/10.1016/j.petrol.2014.08.024.

Thyne, G., Brady, P., 2016. Evaluation of formation water chemistry and scale prediction: Bakken shale. Appl. Geochem. 75, 107–113. https://doi.org/10.1016/j.apgeochem.2016.10.015.

Unsal, E., ten Berge, A.B.G.M., Wever, D.A.Z., 2018. Low salinity polymer flooding: lower polymer retention and improved injectivity. J. Pet. Sci. Eng. 163, 671–682. https://doi.org/10.1016/j.petrol.2017.10.069.

Vermolen, E.C.M., Pingo Almada, M., Wassing, B.M., Ligthelm, D.J., Masalmeh, S.K., 2014. Low-salinity polymer flooding: improving polymer flooding technical feasibility and economics by using low-salinity make-up brine. In: International Petroleum Technology Conference. Society of Petroleum Engineers. https://doi.org/10.2523/IPTC-17342-MS.

Wang, D., Dong, H., Lv, C., Fu, X., Nie, J., 2009. Review of practical experience by polymer flooding at daqing. SPE Reservoir Eval. Eng. 12 (3), 470–476. https://doi.org/10.2118/114342-PA.

Yoo, H., Lee, J., 2020. Impact of design parameters on oil recovery performance in polymer flooding with low-salinity water-flooding. Geosystem Eng 23, 63–72. https://doi.org/10.1080/12269328.2020.1732839.

Yousef, A.A., Al-Saleh, S.H., Al-Kaabi, A., Al-Jawfi, M.S., 2011. Laboratory investigation of the impact of injection-water salinity and ionic content on oil recovery from carbonate reservoirs. SPE Reservoir Eval. Eng. 14 (5), 578–593. https://doi.org/10.2118/137634-PA.

Zaitoun, A., Chauveteau, G., 1998. Effect of pore structure and residual oil on polymer bridging adsorption. In: SPE/DOE Improved Oil Recovery Symposium. Society of Petroleum Engineers. https://doi.org/10.2118/39674-MS.

Zhang, G., Seright, R., 2013. Effect of concentration on HPAM retention in porous media. In: SPE Annual Technical Conference and Exhibition. Society of Petroleum Engineers. https://doi.org/10.2118/166265-MS.

Zhang, S., She, Y., Gu, Y., 2011. Evaluation of polymers as direct thickeners for CO_2 enhanced oil recovery. J. Chem. Eng. Data 56 (4), 1069–1079. https://doi.org/10.1021/je1010449.

Zhu, G., Liu, X., Yang, H., Su, J., Zhu, Y., Wang, Y., Sun, C., 2017. Genesis and distribution of hydrogen sulfide in deep heavy oil of the Halahatang area in the Tarim basin, China. J. Nat. Gas. Geosci. 2 (1), 57–71. https://doi.org/10.1016/j.jnggs.2017.03.004.